The synthesis and structure of a cadmium complex of dimorpholinodithioacetylacetonate and its use as single source precursor for CdS thin films or nanorods†

Karthik Ramasamy, Mohammad A. Malik, Paul O'Brien* and James Raftery

Received 29th September 2008, Accepted 16th December 2008
First published as an Advance Article on the web 5th February 2009
DOI: 10.1039/b816909h

A facile method for the preparation of dimorpholides of dithioacetylacetonate is described together with a X-ray single crystal structure of the ligand and of [Cd(msacmsac)$_2$(NO$_3$)$_2$] (msacmsac = dimorpholinodithioacetylacetonate). The cadmium complex has been used as a single source precursor for the deposition of the CdS thin films by the aerosol assisted chemical vapour deposition (AACVD) method or as nanorods by thermolysis in oleylamine. The thin films and nanorods were characterized by electronic spectra (UV-Vis), photoluminescence (PL), X-ray diffraction (XRD), selected area electron diffraction (SAED), scanning electron microscopy (SEM), and transmission electron microscopy (TEM). To the best of our knowledge [Cd(msacmsac)$_2$(NO$_3$)$_2$] is the first complex in its class to be used as a single source precursor to deposit CdS thin films or nanoparticles.

Introduction

Cadmium sulfide is a group II–VI semiconductor with a direct band gap of 2.42 eV.[1] It is well known to be an important device material as it can be used in solar cells, in light-emitting diodes for flat-panel display, and other devices.[2–4] It has been prepared by various methods such as chemical bath deposition (CBD),[5,6] spray pyrolysis,[7,8] solution growth,[9,10] and metal organic chemical vapour deposition (MOCVD).[11,12] Amongst these techniques the MOCVD method is well known and often gives good quality thin films. A major role in tailoring material properties resides in the choice of the molecular precursors, whose nature can strongly affect the morphology and composition of the final product. In particular, single source precursor containing all the elements to be deposited in a unique molecule[13,14] can be used as convenient building blocks for materials. CdS nanocrystals have been prepared using a wide range of synthetic methods.[15–20] The use of single source precursor for CdS as initially reported by Trindade and O'Brien,[21,22] has also provided an efficient route to high quality crystalline monodispersed nanoparticles of semiconductors. Various single source precursors have been developed including dialkyldithiocarbamates,[23] xanthates,[24,25] N-alkyl thioureas,[26] dithiophosphinates,[12] and dithioimidodiphosphinates,[27] which have been used for the preparation of CdS thin films and nanoparticles. A review by Gleizes gives a detailed account on the use of single source precursors by CVD method.[28] Herein, we report the synthesis of [Cd(msacmsac)$_2$(NO$_3$)$_2$], single crystal X-ray diffraction studies for the ligand and complex, and its use in the deposition of CdS thin films and nanorods.

The School of Chemistry and the School of Materials, The University of Manchester, Oxford Road, Manchester, UK M13 9PL. E-mail: paul.obrien@manchester.ac.uk; Fax: +44 161 275 4598; Tel: +44 161 275 4653

† Electronic supplementary information (ESI) available: Experimental details for CdS thin films and CdS nanorods. CCDC reference numbers 685538 and 685540. For ESI and crystallographic data in CIF or other electronic format see DOI: 10.1039/b816909h

Experimental

All preparations were performed under an inert atmosphere of dry nitrogen using standard Schlenk techniques. All reagents were purchased from Sigma-Aldrich chemical company and used as received. Solvents were distilled prior to use. ^{1}H NMR studies were carried out using a Bruker AC300 FTNMR instrument. Mass spectra were recorded on a Kratos concept 1S instrument. Elemental analysis was performed by the University of Manchester micro-analytical laboratory. Melting points were recorded on a Stuart melting point apparatus and uncorrected.

Synthesis of msacmsac

Morpholine (26.1 g, 2.9 mmol), sulfur (12.8 g, 3.9 mmol), and allyl propylether (5 g, 0.4 mmol) were heated to 110 °C with stirring under nitrogen atmosphere and maintained for 5 h. Progress of the reaction was monitored by TLC. After completion the reaction mixture was cooled to room temperature followed by 50 ml of methanol. Stirring continued for 15 min, the solid product was filtered and washed with methanol. Recrystallisation from acetonitrile yielded colourless needle crystals suitable for single crystal diffraction. Yield: 3.6 g (26%), mp: 208 °C, MS (ES) major peaks m/z = [M$^+$] 274, [$C_{11}H_{18}N_2O_2S$] 241, ^{1}H NMR (200 MHz, $CDCl_3$): δ 3.7–3.9 (m, 12H), 4.3 (m, 4H), 4.38 (s, 2H). Elemental analysis: Found: C, 48.1; H, 6.8; N, 10.2; S, 22.6%. Calc. for $C_{11}H_{18}N_2O_2S_2$: C, 48.2; H, 6.6; N, 10.2; S, 23.3%.

Synthesis of [Cd(msacmsac)$_2$(NO$_3$)$_2$]

Cadmium nitrate (0.281 g 0.9 mmol) was dissolved in 10 ml of acetonitrile and added dropwise to a stirred solution of msacmsac (0.5 g, 1.8 mmol) in anhydrous acetonitrile. The resulting solution was stirred at room temperature for 30 min. The colour of the solution changed to deep yellow upon stirring. The solution was allowed to evaporate in room temperature. After 24 h in room temperature yielded colourless crystals suitable for single

crystal diffraction experiments. Yield: 0.62 g (87%), mp: 88–90 °C, MS (ES) major peaks m/z = [M$^+$] 784.1, [$C_{11}H_{18}N_2O_2S_2$] 274, [$C_{11}H_{18}N_2O_2S$] 241, ^{1}H NMR (200 MHz, $CDCl_3$): δ 3.7–3.9 (m, 12H), 4.3 (m, 4H), 4.38 (s, 2H). Elemental analysis: Found: C, 32.7; H, 4.7; N, 10.4; S, 15.0; Cd, 13.7%. Calc. for $C_{22}H_{36}N_6O_{10}S_4Cd$: C, 33.8; H, 4.6; N, 10.7; S, 16.3; Cd, 14.2%.

Crystal structure determination

Single-crystal X-ray diffraction data for the compounds were collected using graphite monochromated Mo Kα radiation (λ = 0.71073 Å) on a Bruker APEX diffractometer. The structure was solved by direct methods and refined by full-matrix least squares on F^2.[29] All non-H atoms were refined anisotropically. H atoms were included in calculated positions, assigned isotropic thermal parameters and allowed to ride on their parent carbon atoms. All calculations were carried out using the SHELXTL package.[30] CCDC reference numbers 685538 and 685540.†

[msacmsac]

$C_{11}H_{18}N_2O_2S_2$, M = 274.39, colourless needles, monoclinic, space group C_2/c, a = 21.701(4), b = 5.165(9), c = 23.364(4) Å, α = 90, β = 98.890(4), γ = 90°, V = 2587.5(8) A^3, Z = 8, D = 1.409 Mg m^{-3}, T = 100(2) K, reflections collected = 7770/3033, unique reflections = [R_{int} = 0.0558], final R indices [$I > 2\sigma(I)$], R_1 = 0.0550, wR_2 = 0.0909, R indices (all data) = R_1 = 0.1093, wR_2 = 0.1062, largest diff. peak and hole = 0.427 and –0.296 e A^{-3}, GOF = 0.874.

[Cd(msacmsac)$_2$(NO$_3$)$_2$]

$C_{22}H_{36}CdN_6O_{10}S_4$, M = 785.21, yellow plates, triclinic, space group $P\bar{1}$, a = 08.564(2), b = 09.404(2), c = 10.519(3) Å, α = 97.480(4), β = 112.429(3), γ = 100.832(4)°, V = 749.8(3) A^3, Z = 1, D = 1.739 Mg m^{-3}, T = 100(2) K, reflections collected = 6436/3376, unique reflections = [R_{int} = 0.0345], final R indices [$I > 2\sigma(I)$], R_1 = 0.0471, wR_2 = 0.1283, R indices (all data) R_1 = 0.0482, wR_2 = 0.1303, largest diff. peak and hole = 2.813 and –2.132 e A^{-3}, GOF = 1.059.

Deposition of films by AACVD

In a typical deposition, 60 mg (7.7×10^{-3} mmol) of the precursor was dissolved in 10 ml mixture of dimethylformamide and chloroform (1 : 1) in a two-necked 100 ml round-bottom flask with a gas inlet that allowed the carrier gas (argon) to pass into the solution to aid the transport of the aerosol. This flask was connected to the reactor tube by a piece of reinforced tubing. The argon flow rate was controlled by a Platon flow gauge. Seven glass substrates (approx. 1 × 3 cm) were placed inside the reactor tube, which is placed in a Carbolite furnace. The precursor solution in a round-bottom flask was kept in a water bath above the piezoelectric modulator of a Pifco ultrasonic humidifier (Model No. 1077). The aerosol droplets of the precursor thus generated were transferred into the hot wall zone of the reactor by carrier gas. Both the solvent and the precursor were evaporated and the precursor vapor reached the heated substrate surface where thermally induced reactions and film deposition took place.

Synthesis of CdS nanorods

In a three-neck flask [Cd(msacmsac)$_2$(NO$_3$)$_2$] (0.5 g) was dissolved in 15 ml of oleylamine and heated to 160 °C under nitrogen flow. Heating was continued for 2 h. The solution was cooled to 60 °C and excess of dry methanol was added. The precipitate formed was centrifuged and clear solution decanted. The precipitate was washed twice with methanol to remove excess oleylamine. Reactions were repeated under different conditions to investigate the changes in size and the shape of the CdS nanorods.

Characterization of thin films and nanorods

X-Ray diffraction studies were performed on a Bruker AXS D8 diffractometer using Cu Kα radiation. The samples were mounted flat and scanned between 20 to 80 °C in a step size of 0.05 with a count rate of 9 s. Films were carbon coated using Edward's E306A coating system before carrying out SEM and EDAX analyses. SEM analysis was performed using a Philips XL 30FEG and EDAX was carried out using a DX4 instrument. TEM analysis was performed using a cm200 instrument. UV-Vis spectra were measured using a Heλios-BetaThermospectronic spectrophotometer. Photoluminescence spectra were measured using a Gilton fluorosens spectroflurometer.

Results and discussion

A schematic diagram for the stepwise synthesis of the ligand, its cadmium complex and the growth of nanoparticles and thin films is given in Fig. 1. The ligand was recrystallised from acetonitrile at room temperature to give transparent needles suitable for X-ray crystallography. The structure of the ligand shows that the sulfur atoms are *trans* to each other. Martin and Stewart[31] observed that the similar SacSac ligand does not exist as uncyclized. In contrast to this observation we have isolated the linear monomeric morpholine substituted SacSac ligand (Fig. 2). The reason may be

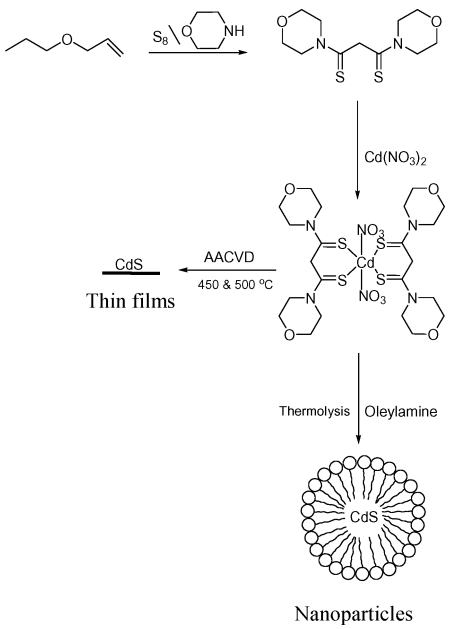

Fig. 1 Schematic representation of preparation of ligand, precursor, CdS thin films and nanorods.

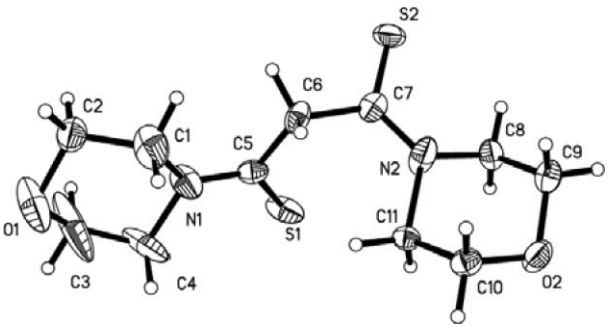

Fig. 2 Molecular structure of [msacmsac] with thermal ellipsoids plotted at the 50% probability. Selected bond distances (Å) and angles (°): C5–S1 = 1.665(3), C5–N1 = 1.320(3), C5–C6 = 1.510(3), O1–C2 = 1.472(4), C6–C5–S1 = 120.5(2), C5–N1–C4 = 120.6(3).

the steric hindrance caused by morpholine rings. Both morpholine rings are disordered and have been modelled so each ring has one alternative conformation in the ratio of 74 : 26 and 49 : 51 for the rings containing N1 and N2 respectively. Crystal data and refinement parameters are given in the crystal structure determination section and important bond lengths and bond angles are given in Fig. 2 caption.

[Cd(msacmsac)$_2$(NO$_3$)$_2$]

The crystal structure of [Cd(msacmsac)$_2$(NO$_3$)$_2$] is shown in Fig. 3. The lone pair at the sulfur is responsible for the formation of the six membered chelate ring with a strong Cd–S bond. Two molecules of the bidentate msacmsac ligand are coordinated to cadmium through lone pair of electrons at sulfur atoms equatorially and axial bonds are formed through the oxygen atoms of nitrate group to complete the octahedral coordination. The axial compression of Cd–O (2.385 Å) makes the molecule unusually elongated Cd–S (2.628–2.699 Å). The coordination is similar to that observed in dithiomalonamides of antimony.[32] The morpholine rings maintain their chair conformation. The morpholine rings maintain their chair conformation. Crystal data and refinement parameters for [Cd(msacmsac)$_2$(NO$_3$)$_2$] are given in the crystal structure determination section and important bond lengths and bond angles are given in Fig. 3 caption.

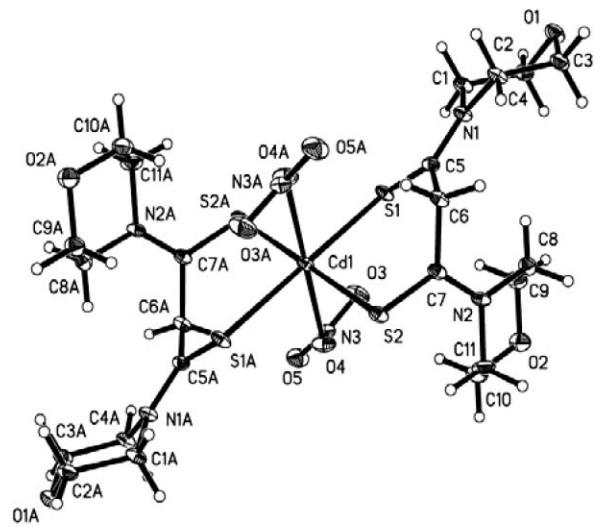

Fig. 3 Molecular structure of [Cd(msacmsac)$_2$(NO$_3$)$_2$] with thermal ellipsoids plotted at the 50% probability. Selected bond distances (Å) and angles (°): Cd1–S2 = 2.6286(9), Cd1–S1 = 2.6992(9), Cd1–O4 = 2.385(2), N3–O3 = 1.234(4), N3–O5 = 1.245(3), O4–Cd1–S2 = 91.72(6), S2–Cd1–S1 = 95.91(2).

Thin films

CdS thin film depositions were carried out as a function of temperature. Very thin films were obtained at the lowest temperature of 450 °C. Thicker films were obtainable at the higher temperatures.

Characterizations of CdS films

Standard q-2q scans cannot always reliably distinguish (111)-oriented cubic CdS from hexagonal CdS with (001).[33] However, in this study XRD produced no real evidence for cubic CdS in any films. The three dominant peaks in most diffraction patterns from films grown at 450 °C can be assigned to the CdS (100), (002), (101) reflections of hexagonal phase which are also the three strongest peaks in the powder pattern. Films grown on glass at 500 °C show preferred orientation along the (101) plane (Fig. 4).

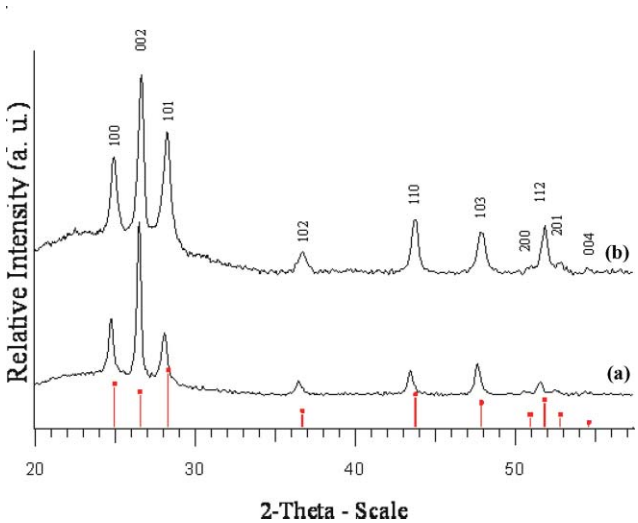

Fig. 4 X-Ray diffraction patterns of CdS thin films grown on glass at (a) 450 °C, (b) 500 °C. Solid lines representing the hexagonal phase (JCPDS-0772306).

SEM images given in Fig. 5 exhibit clusters of crystallites for films deposited at 450 °C and 500 °C. These films comprise of different sizes of clusters formed by granular crystallites ranging from 0.9 to 1.3 μm. The bigger clusters probably grown by fusion

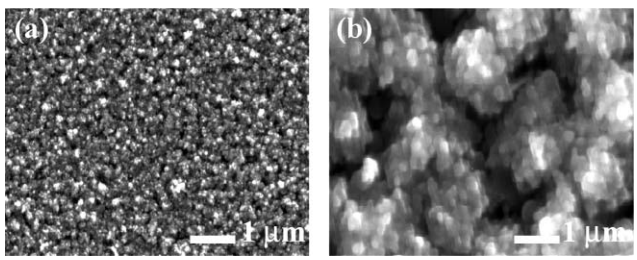

Fig. 5 SEM micrographs of CdS thin films grown on glass at (a) 450 °C and (b) 500 °C. Bar = 1 μm.

of smaller clusters. The granular crystallites of CdS grown on glass substrates at 500 °C are considerably larger than those grown at 450 °C. EDAX analysis confirms the CdS composition close to 1 : 1 at 450 °C (Cd, 53; S, 47%) but sulfur deficient films were obtained at 500 °C (Cd, 55; S, 45%).

CdS nanorods

The shape control of inorganic nanocrystals is topical in nanoscience.[34] The crystalline phase of seeds at the nucleating stage can be critical in directing the intrinsic shape of the nanocrystals due to its characteristic unit cell structure. At this stage, the crystalline phase of the seed can be highly dependent on reaction environment, especially temperature. The XRD pattern (Fig. 6) of CdS nanocrystals shows the hexagonal phase (JCPDS-0772306). The growth at 200 °C and 240 °C shows that the crystallites are elongated along the *c*-axis. In general higher the reaction temperature stronger and narrower the XRD peaks, concurrent with the increase in mean size of the nanocrystals.

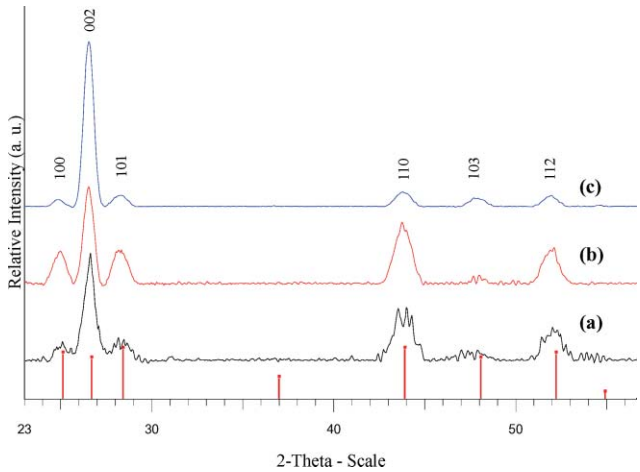

Fig. 6 Powder X-ray diffraction patterns of CdS nanorods grown at (a) 160 °C, (b) 200 °C and (c) 240 °C. Solid lines representing the hexagonal phase (JCPDS-0772306).

TEM images of CdS nanorods are shown in Fig. 7. The nanorods grown at 160 °C show a mixture of spherical particles, double armed rods, and single armed rods. As the temperature increased to 200 °C, nanocrystals formed tripods and bipods. At 240 °C the formation of rods dominated and the aspect ratio of the nanorods decreased. This observation is consistent with earlier results.[35] HRTEM images of the nanorods are shown in Fig. 7(d) and have lattice fringes with a *d*-spacing 0.337 nm corresponding to (002) reflection. SAED pattern consist of broad diffuse rings, which are indicative of the small size of rods. The diffraction rings can be indexed to the (002), (110), (103) and (112) planes of the wurzite phase.

The UV-Vis spectra for as synthesized CdS nanorods are shown in Fig. 8(a–c). The band edges were close to each other for all the samples at 160 °C (500 nm), 200 °C (505 nm) and 240 °C (509 nm).

When the size of CdS nanocrystals becomes smaller than the exciton radius, quantum size effects lead to a size dependent increase in the band gap and a blue-shift in the absorption onset.[36] The increment in band gap is approximately inversely proportional to the square of the crystal size based on the effective mass

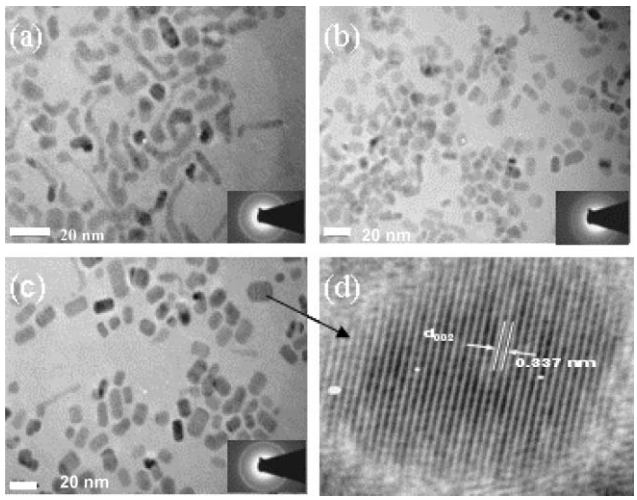

Fig. 7 TEM image and SAED pattern of CdS nanocrystals synthesized at (a) 160 °C, (b) 200 °C and (c) 240 °C; (d) HRTEM image of CdS nanorods at 240 °C.

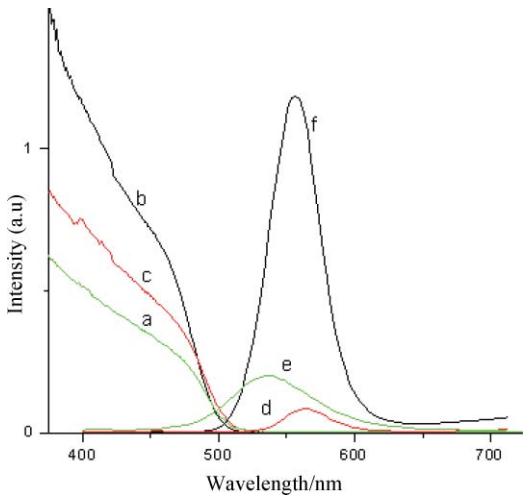

Fig. 8 Absorption spectra (a–c) and photoluminescence spectra (d–f) (372 nm excitation) for CdS nanorods grown at 160 °C, 200 °C and 240 °C respectively.

approximation.[37] It is well known that the absorption spectrum can characterize the dispersivity of the nanoparticles.[38] The spectra of samples grown at 160 °C, 200 °C and 240 °C show clear absorption peaks. But at higher temperatures the absorption tail is prolonged suggesting deterioration of the dispersivity with the increase in the size of nanoparticles. The size of the particles was also investigated by using the Wang equation.[39] The nanoparticles grown at 160 °C, 200 °C and 240 °C showed only a slight change in size 7.7, 8.0 and 8.2 nm respectively.

Photoluminescence measurements were carried out at room temperature with an excitation wavelength 372 nm. Photoluminescence spectra in toluene solution of CdS nanorods are shown in Fig. 8(d–f). Emission peaks were observed near the band edges at 492 nm, 484 nm and 496 nm for samples grown at 160 °C, 200 °C and 240 °C respectively. The photoluminescence appears to increase by the increase in growth temperature. The highest photoluminescence was observed for the nanorods grown at 240 °C. The nanorods grown at this temperature contain only

the rods without any mixture of bipods or tripods as observed for samples grown at 200 °C or 160 °C.

Conclusion

The crystal structure of $[Cd(msacmsac)_2(NO_3)_2]$ shows a bidentate coordination by the sulfur atoms of each ligand. The coordination geometry around cadmium is close to octahedral. Deposition of thin films at various temperatures showed the growth of CdS clusters which were made of granular crystallites. The cluster size increased by increasing the deposition temperatures. Thermolysis of the precursor in oleylamine at 160–240 °C gave nanorods with hexagonal phase of CdS. The band edges of the nanorods grown at different temperature were similar but more intense photoluminescence was observed for samples grown at 240 °C.

Acknowledgements

KR is grateful to ORS and The University of Manchester for financial support. The authors also thank EPSRC, UK for the grants to POB that have made this research possible.

Notes and references

1 K. W. Seo, S. H. Yoon, S. S. Lee and I. W. Shim, *Bull. Korean Chem. Soc.*, 2005, **26**, 1582.
2 I. P. Deshmuhk, S. G. Holikatti and P. P. Hankare, *J. Phys. D: Appl. Phys.*, 1996, **27**, 1784.
3 G. Z. Shen and C. J. Lee, *Cryst. Growth Des.*, 2005, **5**, 1085.
4 Z. L. Wang, *Adv. Mater.*, 2000, **12**, 1295.
5 U. Gangopadhyay, K. Kim, D. Mangalaraj and Yi, *Appl. Surf. Sci.*, 2004, **230**, 364.
6 S. Kundu and L. C. Olsen, *Thin Solid Films*, 2005, **471**, 298.
7 A. Ashour, H. H. Afifi and S. A. Mahmoud, *Thin Solid Films*, 1994, **248**, 253.
8 R. D. Pike, H. Cui, R. Kershaw, K. Dwight, A. Wold, T. N. Blanton, A. A. Wernberg and H. Gysling, *Thin Solid Films*, 1993, **224**, 221.
9 I. C. Ndukwe, *Sol. Energy Mater. Sol. Cells*, 1996, **40**, 123.
10 J. Lee, S. Lee, S. Cho, S. Kim, I. Y. Park and Y. D. Choi, *Mater. Chem. Phys.*, 2002, **77**, 254.
11 H. Kashani, *Thin Solid Films*, 1996, **288**, 50.
12 C. Byrom, M. A. Malik, P. O'Brien, A. J. P. White and D. J. Williams, *Polyhedron*, 2000, **19**, 211.
13 F. Maury, *Chem. Vap. Deposition*, 1996, **2**, 113.
14 A. N. Gleizes, *Chem. Vap. Deposition*, 2000, **6**, 115.
15 H. Weller, *Adv. Mater.*, 1993, **5**, 88.
16 A. Hagfeldt and M. Gratzell, *Chem. Rev.*, 1995, **95**, 49.
17 R. Rossetti, J. L. Ellison, J. M. Gibson and L. E. Brus, *J. Chem. Phys.*, 1984, **80**, 4464.
18 A. Henglein, *Chem. Rev.*, 1989, **89**, 1861.
19 M. L. Steigerwald and L. E. Brus, *Acc. Chem. Res.*, 1990, **23**, 183.
20 Y. Wang and N. Herron, *J. Phys. Chem.*, 1991, **95**, 525.
21 T. Trindade and P. O'Brien, *Adv. Mater.*, 1996, **8**, 161.
22 T. Trindade and P. O'Brien, *Chem. Mater.*, 1997, **9**, 523.
23 A. A. Memon, M. Afzaal, M. A. Malik, C. Q. Nguyen, P. O'Brien and J. Raftery, *Dalton Trans.*, 2006, 4499.
24 P. S. Nair, T. Radhakrishnan, N. Revaprasadu, G. Kolawole and P. O'Brien, *J. Mater. Chem.*, 2002, **12**, 2722.
25 D. Barreca, A. Gasparotto, C. Maragno, R. Seraglia, E. Tondello, A. Venzo, V. Krishnan and H. Bertagnolli, *Appl. Organomet. Chem.*, 2005, **19**, 59.
26 M. J. Moloto, P. O'Brien, M. A. Malik and N. Revaprasadu, *J. Mater. Sci.: Mater. Electron.*, 2004, **15**, 313.
27 Dongbo Fan, Mohammad Afzaal, M. Azad Mallik, Chinh Q. Nguyen, Paul O'Brien and P. John Thomas, *Coord. Chem. Rev.*, 2007, **251**, 1878–1888.
28 A. N. Gleizes, *Chem. Vap. Deposition*, 2000, **6**, 155.
29 G. M. Sheldrick, *SHELXS-97, Program for solution of crystal structures*, University of Göttingen, Germany, 1997; G. M. Sheldrick, *SHELXL-97, Program for refinement of crystal structures*, University of Göttingen, Germany, 1997.
30 Bruker, *SHELXTL* Version 6.12, Bruker AXS Inc., Madison, Wisconsin, USA, 2001.
31 R. L. Martin and I. M. Stewart, *Nature*, 1966, **210**, 522.
32 J. M. Kisenyi, G. R. Wiley and M. G. B. Drew, *J. Chem. Soc., Dalton Trans.*, 1985, 1073.
33 JCPDS Powder Diffraction File Entries 6-314, hexagonal CdS (greenockite), and 10-454, cubic CdS (hawleyite).
34 S. M. Lee, S. N. Cho and J. W. Cheon, *Adv. Mater.*, 2003, **15**, 441.
35 Y. Li, X. Li, C. Yang and Y. Li, *J. Mater. Chem.*, 2003, **13**, 2641.
36 P. Sreekumari Nair, T. Radhakrishnan, N. Revaprasadu, G. A. Kolawole and P. O'Brien, *Polyhedron*, 2003, **22**, 3129.
37 L. E. Brus, *J. Phys. Chem.*, 1986, **90**, 2555.
38 S. Modes and P. Lianos, *J. Phys. Chem.*, 1989, **93**, 5854.
39 Y. Wang, A. Suna, W. Mahler and R. Kasowski, *J. Chem. Phys.*, 1987, **87**, 73115.

